Inhibition Effects of Amides on the Corrosion of Copper in 1.0 M HCl: Theoretical and Experimental Studies

S. Zor, M. Saracoglu,‡,** F. Kandemirli,*** and T. Arslan*****

ABSTRACT

The corrosion inhibition effects of benzamide (BA) and 4-aminobenzenesulfonamide (ABSA) for copper in 1.0 M hydrochloric acid (HCl) solution were investigated using potentiodynamic polarization, cyclic voltammetry (CV), and potentiostatic current-time curves. The Langmuir adsorption isotherms of the inhibitors were used to explain the adsorption behavior. In addition, surface analysis of copper was investigated using scanning electron microscopy (SEM). The results showed that the inhibition efficiency of ABSA was much better than those of BA. The theoretical study on the corrosion inhibition efficiencies for neutral and protonated forms of the BA and ABSA molecules were performed using density functional theory (DFT) and MP2 method in gas and water phases.

KEY WORDS: acid solutions, copper, corrosion, polarization

INTRODUCTION

Copper and its alloys are commonly used as a material in industrial systems because of their excellent electrical and thermal conductivity, good corrosion resistance, and mechanical workability.[1] They are used widely in many applications in electronic industries and communications as a conductor in electrical power lines, and in pipelines for domestic and industrial water utilities including seawater, heat conductors, heat exchangers, etc.[1-10] Therefore, corrosion of copper and its inhibition in a wide variety of media, particularly when they contain chloride ions in high concentrations, have attracted the attention of many investigators.[11] It is known that the mechanism of copper electrodeposition/dissolution strongly depends on the medium.[4] It is generally accepted that anodic dissolution of copper is influenced by chloride concentration independently of pH.[12] The dissolution of copper at lower than 1.0 M chloride concentration occurs through formation of copper(I) chloride (CuCl), which is not protective and then is converted to the soluble copper chloride complex ($CuCl_2^-$) by reacting with an excess of chloride. At chloride concentrations higher than 1.0 M, higher cuprous complexes such as $CuCl_3^{2-}$ and $CuCl_4^{3-}$ and fewer chlorides complexes such as CuCl and $CuCl_2^-$ are formed.[12-13]

The use of inhibitors is one of the most practical methods of protection against corrosion, especially in acidic media.[2-15] Inhibitors are commonly used in these processes to control the metal dissolution as well as acid consumption.[3] The most acid corrosion inhibitors are nitrogen-sulfur and oxygen-containing organic compounds.[2-7] Among these organic compounds, the azole derivatives are also most commonly used. Benzotriazole (BTA) is well known as an effective inhibitor of copper corrosion in neutral/alkaline solutions.[11-16] BTA and its derivatives have been used in industry widely for several decades.[16-23] However, a very important deficiency of these inhibitors is their toxicity and most them are not biodegradable. BTA also does not show a high inhibiting effect on

Submitted for publication February 15, 2011; in revised form, June 28, 2011.

‡ Corresponding author. E-mail: muratsaracoglu@gmail.com; saracm@erciyes.edu.tr.
* Department of Chemistry, Kocaeli University, 41000 Izmit, Turkey.
** Faculty of Education, Erciyes University, 38039 Kayseri, Turkey.
*** Department of Chemistry, Niğde University, 51240 Niğde, Turkey.
**** Department of Chemistry, Eskişehir Osmangazi University, 26480 Eskişehir, Turkey.

ISSN 0011-9312 (print), 1938-159X (online)
11/000155/$5.00+$0.50/0 © 2011, NACE International

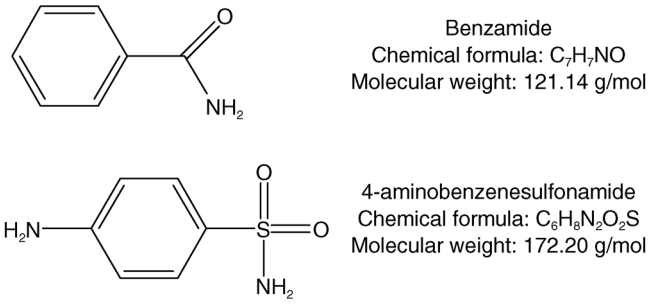


FIGURE 1. *Structure of inhibitor molecules.*

copper corrosion in acidic solution.[11] Therefore, their replacement by new, non-toxic inhibitors is desirable.[24-27] Amides are described as organic molecules containing the group of $–NH_2$. Some amides contain atoms with high electron levels, such as N, O, and S in their molecular structures. Amide and derivatives are of particular importance as corrosion inhibitors, because they are environmentally friendly and have very low toxicity. The inhibition efficiencies of amides on steel have generally been studied in the literature. For instance, urea (U), thiourea (TU), thioacetamide (TA), and thiosemicarbazide (TSC) have been found to be good inhibitors for mild steel in acid solutions.[13-17] However, inhibition effects of amides on copper in literature have not been studied much.[18]

The performance of the organic inhibitors can be interpreted in terms of the structure of the molecule, molecular size, and nature of the heteroatoms present in the molecule. Makrides and Hackermann[28] proposed that sulfur-containing organic compounds have special efficacy since these compounds are better electron donors. The inhibition performance of ABSA is better than BA because of the presence of increased electron density at active centers in the inhibitor molecule containing both sulfur and nitrogen atoms. The higher inhibition efficiency observed with ABSA containing both nitrogen and sulfur atoms are attributed to the presence of a higher number of lone pairs of electrons, and a higher polarizability.[11]

In the present study, efficiency of amides for inhibition of copper corrosion in acidic solution was investigated. The goal of this work was to examine the effectiveness of amides to suppress the corrosion of copper in acidic solution. The performance of the inhibitors was evaluated using various electrochemical techniques.

There are several quantum chemical studies to investigate the relationship between the corrosion inhibition efficiency and inhibitor quantum-chemical parameters such as: the HOMO (highest occupied molecular orbital), LUMO (lowest unoccupied molecular orbital), energy polarizability, charges, hardness (η), softness (σ), electronegativity (χ), etc.[29-34]

EXPERIMENTAL PROCEDURES

Electrochemical Measurements

The electrolyte solution was made from HCl and distilled water. Benzamide (BA) and 4-aminobenzenesulfonamide (ABSA) were used as inhibitors. The inhibitors were used as-received. The molecular structures of the studied inhibitors are shown in Figure 1.

All experiments were carried out in an 200 mL electrochemical cell with a three-electrode configuration at room temperature with the electrolyte solution in equilibrium with the atmosphere (aerated solutions). The working electrode (WE) was prepared from a cylindrical copper rod (99.99%) sealed with epoxy resin so that only the circular cross section (0.785 cm^2) of the rod was exposed to the corrosion. A saturated calomel electrode (SCE) was used as the reference electrode with a fine Luggin capillary positioned close to the working electrode surface to minimize the ohmic potential drop. A platinum wire was used as a counter electrode (CE). Prior to the electrochemical measurements, the WE was abraded with emery papers (grades 320, 400, 800, and 1200), washed with distilled water, degreased with acetone (CH_3COCH_3), washed with distilled water again, dried at room temperature, and finally immersed into the cell. The electrode potential was allowed to stabilize for 60 min before starting the measurements.

Electrochemical measurements were performed by using a potentiostat/galvanostat. Potentiodynamic polarization curves were obtained by changing the electrode potential automatically from –0.70 V to 0.10 V at a scan rate of 5 mV s^{-1}. All potentials were measured against the saturated calomel electrode (SCE). Potentiostatic current-time experiments were carried out by stepping the potential at 0.25 V for 60 min. Cyclic voltammetry curves were obtained in 1.0 M hydrochloric acid (HCl) with and without inhibitor. The working electrode was scanned from negative to positive in the potential range from –0.6 V to 0.6 V, at a scan rate of 20 mV s^{-1}.

Scanning Electron Microscopic Study

The copper specimens were immersed in 1.0 M HCl with and without inhibitor solutions for a period of 7 days. After 7 days, the specimens were taken out and dried. The nature of the film formed on the surface of metal specimens was analyzed using scanning electron microscopy (SEM). Metal surfaces were investigated using a scanning electron microscope.

Calculation Method

The molecular sketches of the compounds BA and ABSA were drawn using the GaussView 5.0[†]. All the quantum chemical calculations were performed with complete geometry optimizations using a standard Gaussian-09[†] software package.[35] The Becke's three-parameter hybrid functional[36-38] combined with

[†] Trade name.

the Lee, Yang, and Parr (LYP) correlation functional[39] and denoted as B3LYP was used in the density functional theory (DFT) calculations using the 6-31G(d,p) and 6-311G(d,p) basis set levels for geometry optimizations and quantum chemical calculations. MP2 calculations were also performed with 6-31G(d,p) and 6-311G(d,p) basis set levels. Fukui functions were calculated with the AOMix† program[40-41] using single-point calculations at the B3LYP/6-311G(d,p) level of theory. The integral equation formalism-polarizable continuum model (IEF-PCM) method, which is a PCM calculation using the integral equation formalism model, was used for water phase calculations.[35]

RESULTS AND DISCUSSION

Cyclic Voltammetric Study

The cyclic voltammogram curves obtained from 5×10^{-3} M BA and ABSA containing or not containing inhibitor in 1.0 M HCl are given in Figure 2. In the curves, two anodic current peaks at about 0.07 V and 0.20 V and one cathodic current peak at –0.225 V can be observed. According to Crundwell and Brusic, et al.,[42-43] the mechanism of dissolution of copper in HCl solutions is:

$$Cu + Cl^- \rightleftarrows CuCl_{ads} + e^- \quad (1)$$

$$CuCl_{ads} + Cl^- \rightleftarrows CuCl_2^- \quad (2)$$

The first oxidation peak can be related to the anodic dissolution of copper occurs by Reaction (1). Under this condition, Cu reacts fast with Cl^-, forming CuCl, which has poor adhesion to the copper surface and is transformed to the soluble cuprous chloride complex, $CuCl_2^-$. The anodic copper dissolution was controlled by both electrodissolution of copper and diffusion of soluble $CuCl_2^-$ to the bulk solution.[44] The second oxidation peak represents the oxidation of Cu(I) to soluble Cu^{2+} by Reaction (4). In the reverse sweep, the corrosion product of CuCl can be partially reduced as described in Reaction (3), as a result of increasing the concentration of Cl^- at the interface of the copper and salt layer, which leads to fast dissolution of copper by Reaction (1).[17]

$$CuCl_{ads} + e^- \rightleftarrows Cu + Cl^- \quad (3)$$

$$CuCl_2^- \rightleftarrows Cu^{2+} + 2Cl^- + e^- \quad (4)$$

On the other hand, the corrosion process would be restrained to a certain extent by increasing the salt layer. Because of the competition of dissolution and precipitation of the film on copper, an anodic current hump appears in the cyclic voltammetry (CV) plot on the reverse sweep at about 0.05 V.[17] The decrease in anodic current between 0 and ~0.05 V was attributed to the formation of partly inhibiting CuCl film on the copper surface (Figure 2). It can be seen that the presence of BA and ABSA causes a decrease in the current density of the first anodic peak. It indicates that BA and ABSA can effectively inhibit the Cu(I) oxidation. Also, the decreases in anodic current of inhibitors are a result of the decreased chloride ion attack on the copper surface by inhibitor molecule adsorption. The results show that BA and ABSA are effective inhibitors for copper.

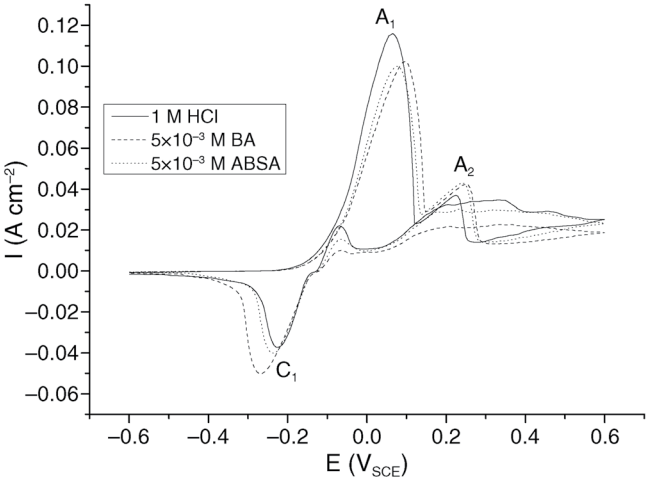


FIGURE 2. *CV curves of copper in 1.0 M HCl with and without inhibitor.*

Potentiodynamic Polarization Measurements

The potentiodynamic polarization curves in 1.0 M HCl in the presence and absence of BA and ABSA at different concentrations are given in Figures 3 and 4, respectively. It is seen clearly from Figures 3 and 4 that the anodic branch of Cu in HCl solutions in the absence of inhibitor molecules shows three distinct regions:

—First, increasing the current from the Tafel region at lower overpotentials, which extending to the maximum current density (I_{max}) as a result of the fast dissolution of Cu^o into Cu^+ (Reaction [5]):

$$Cu \rightleftarrows Cu^+ + e^- \quad (5)$$

—Second, the region of decreasing currents until a minimum (I_{min}) is reached because of the formation of CuCl (Reaction [1]).

—Finally, the region of sudden increase in current density leads to a limiting value (I_{lim}), which is from the presence of acidic solutions that decreases the adhesion properties of the adsorbed CuCl later and leads to the formation of soluble copper chloride complex, $CuCl_2^-$ (Reaction [2]).[11,15]

The cathodic polarization curves displayed a current plateau from –0.40 V to –0.60 V, which may be

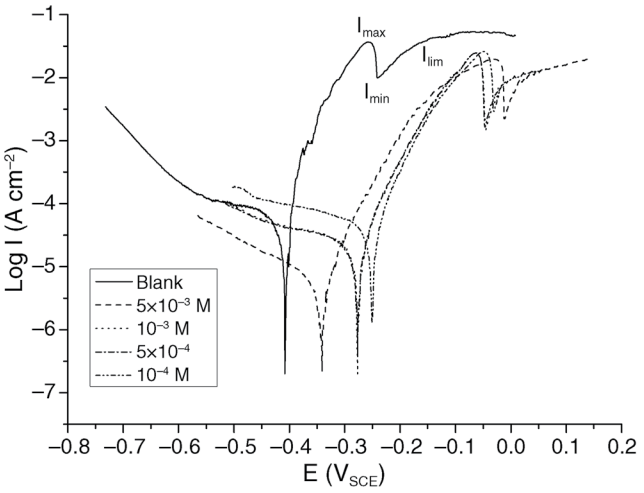


FIGURE 3. *Polarization curves of copper in 1.0 M HCl in the absence and presence of BA.*

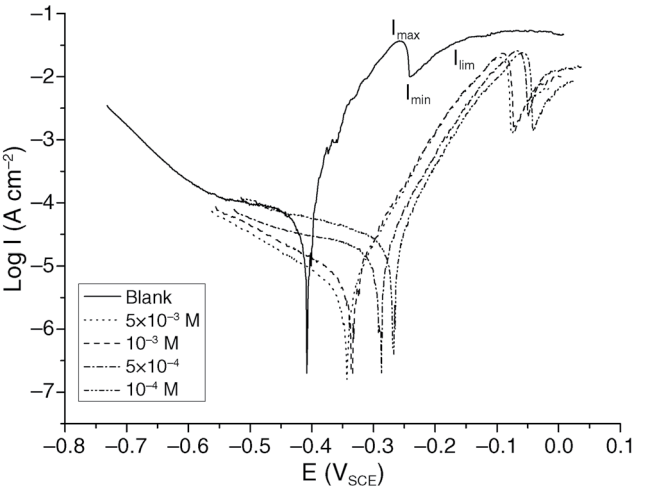


FIGURE 4. *Polarization curves of copper in 1.0 M HCl in the absence and presence of ABSA.*

TABLE 1

Electrochemical Polarization Parameters for Copper in 1.0 M HCl Without and With Inhibitors

C (M)	I_{corr} (μA cm^{-2})	$-E_{corr}$ (mV)	IE%	b_a (mV dec^{-1})	R_p (kΩ·cm^2)
1.0 M HCl	58.0	416.5	—	99	512
10^{-4} M ABSA	24.5	267.8	57.7	65	866
5×10^{-4} M ABSA	19.1	293.6	67.1	60	1,022
10^{-3} M ABSA	10.3	335.8	81.8	74	2,454
5×10^{-3} M ABSA	5.8	344.0	90	62	3,606
10^{-4} M BA	31.7	249.2	45.3	78	776
5×10^{-4} M BA	28.3	280.5	51.2	75	835
10^{-3} M BA	16.8	274.6	71.04	54	1,073
5×10^{-3} M BA	10.7	346.0	81.4	63	1,970

attributed to the diffusion-controlled reduction of dissolved oxygen (Figures 3 and 4). According to Zhang, et al.,[14-17] the cathodic corrosion reaction in an aerated acidic chloride solution is:

$$4H^+ + O_2 + 4e^- \rightleftarrows 2H_2O \quad (6)$$

Also, the total corrosion reaction of copper in acidic chloride solutions is as follows:[15]

$$2Cu + 4H^+ + 4Cl^- + O_2 \rightarrow 2Cu^{2+} + 4Cl^- + 2H_2O \quad (7)$$

In both inhibitors, the anodic and cathodic current density is decreased by adding an inhibitor. Therefore, BA and ABSA acts as mixed-type inhibitors. However, the rate of anodic reaction was decreased more than the cathodic reaction rate and corrosion potential was moved to more positive values compared with 1.0 M HCl (Figures 3 and 4). Accordingly, it was determined that benzamide and sulfanilamide prevent the anodic dissolution of copper.

The corrosion parameters, corrosion potential (E_{corr}) and corrosion current density (I_{corr}), of the metal in the presence of different concentrations of amides were calculated from the potentiodynamic polarization curves. The corrosion parameters (E_{corr}, I_{corr}, b_a, R_p) of the metal in 1.0 M HCl solution with and without inhibitors are given in Table 1.

The inhibition efficiency (IE%) was calculated using the equation:

$$IE\% = \frac{(I_{corr})_0 - (I_{corr})_{inh}}{(I_{corr})_0} \times 100 \quad (8)$$

where $(I_{corr})_0$, $(I_{corr})_{inh}$ are uninhibited and inhibited corrosion current densities, respectively.

As seen in the table, the corrosion potentials of the inhibitors have shifted to more positive values compared to 1.0 M HCl. However, in both inhibitors, corrosion potential shifts to the negative side as the inhibitor concentration increases. The protection of amides for copper is very weak at low concentrations. It can be seen that with increasing inhibitor concentration, corrosion current density decreases. At the same time, the increase of IE% with inhibitor concentration also confirms that BA and ABSA are good

inhibitors and protects the copper surface against corrosion in aerated acidic chloride solutions. Since the sulfur compounds are more polarizable, the inhibition effectiveness of ABSA is more than BA (Table 1).

The polarization resistance (R_p) values are related to the corrosion current density (I_{corr}), which is directly proportional to the corrosion rate, through the Stern-Geary equation:

$$R_p = \frac{b_a \times b_c}{2.303 \times (b_a + b_c)} \times \frac{1}{I_{corr}} \quad (9)$$

The R_p values listed in Table 1 are used to estimate the corrosion inhibition effect of the inhibitors. The addition of BA or ABSA to the acidic solutions produced higher R_p values than the blank solution, indicating the formation of a protective layer on the electrode surface (Table 1). As a result, inhibitors show an inhibitive effect on the anodic dissolution of copper.

Current-Time Measurements

To shed more light on the effects of BA and ABSA on the inhibition of copper corrosion at 0.25 V, potentiostatic current-time measurements were carried out. The variation of current values of copper electrode with time at 0.25 V in 1.0 M HCl with and without inhibitor is shown in Figure 5. The highest current values are observed in 1.0 M HCl solution. In 1.0 M HCl solution, the current decreases from ~38 mA cm^{-2} to ~28 mA cm^{-2} after 60 min. Addition of inhibitors to the chloride solutions decreases the currents with time in solutions to reach to ~16 mA cm^{-2} and 8 mA cm^{-2} in 60 min for copper in BA and ABSA solutions, respectively (Figure 5).

The higher values of current vs. time at 0.25 V for copper in HCl solution without inhibitor is because of the aggressiveness of Cl^- (Figure 5). According to Sherif and coworkers, the decrease in the current with time can be explained since their studies in which the x-ray photoelectron (XPS) and the energy-dispersive x-ray analyzer (EDX) investigations for the copper at similar conditions have shown that only Cu, Cl, and O existed on the surface.[11,45] The possible corrosion products formed on the copper surface may be CuCl (Reaction [1]), $CuCl_2^-$ (Equation [2]), and Cu_2O (Equation [10]),

$$2CuCl + H_2O \rightleftarrows Cu_2O + 2H^+ + 2Cl^- \quad (10)$$

and/or a top layer of sparingly soluble atacamite, $Cu_2(OH)_3Cl$.

$$Cu_2O + Cl^- + 2H_2O \rightleftarrows Cu_2(OH)_3Cl + H^+ + 2e^- \quad (11)$$

The formation of these corrosion products on the copper surface partially protects it and results in decreasing the current values. The decrease of current values by the presence of BA and ABSA are because of the adsorption of amide molecules onto the copper surface, preventing the formation of cuprous chloride and oxychloride complexes, and results in decreasing the chloride ion attack on the copper surface.[1,17]

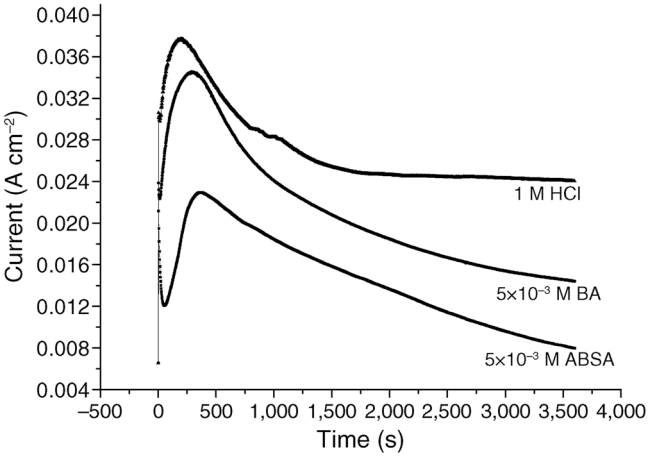


FIGURE 5. *Current-time curves of copper in 1.0 M HCl with and without inhibitor.*

Adsorption Isotherms

To understand the mechanism of corrosion inhibition, the adsorption behavior of the organic adsorbate on the metal surface must be known. The adsorption process of inhibitors are influenced by the chemical structures of organic compounds, the nature and surface charge of metal, and the distribution of charge in molecule on the type of aggressive media.[46]

Basic information on the interaction between the inhibitor and the Cu surface can be provided by the adsorption isotherm. The simplest, being Langmuir isotherm, is based on the assumption that all adsorption sites are equivalent and that particle binding occurs independently from nearby sites being occupied or not. Langmuir isotherm can be expressed as:[47-49]

$$\frac{C}{\theta} = \frac{1}{K_{ads}} + C \quad (12)$$

where C is the inhibitor concentration, K_{ads} (M^{-1}) is the adsorption equilibrium constant, and θ is the surface coverage. In this case, θ is numerically identical to the value of percentage inhibition efficiency obtained from polarization divided by 100: $\theta = \frac{IE\%}{100}$.[48] A typical plot of C/θ vs. C for amides is given in Figure 6. The equilibrium constants of the adsorption process were found from the obtained straight lines in C/θ vs. C graphs and are related to the free energy of adsorption (ΔG^0_{ads}), Equation (13):

$$K_{ads} = \frac{1}{55.5} \times \exp\left(-\frac{\Delta G^0_{ads}}{RT}\right) \quad (13)$$

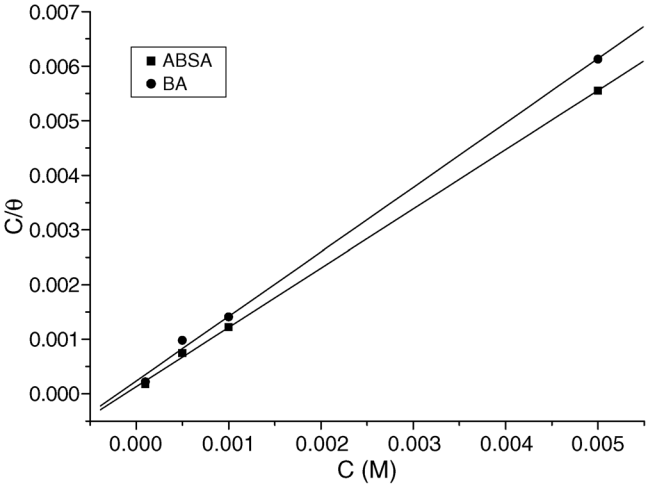


FIGURE 6. *Langmuir adsorption isotherm curves for inhibitor molecules.*

where R is the universal gas constant and T is the thermodynamic temperature. The following values of K_{ads}, 4,214 and 7,575 (M^{-1}) for BA and ABSA, respectively, were obtained. The value of K_{ads}, which indicates the binding power of the inhibitor to the copper surface, can lead to the calculation of the adsorption of free energy. The following values of ΔG^0_{ads}, –30.628 kJ/mol and –32.08 kJ/mol for BA and ABSA, respectively, were obtained. The negative value of ΔG^0_{ads} indicates that the inhibitor is adsorbed spontaneously on the copper surface.[47-51]

It is well known that values of ΔG^0_{ads} in the order of –20 kJ mol^{-1} or lower indicate a physisorption; those about –40 kJ mol^{-1} or higher involve charge sharing or a transfer from the inhibitor molecules to the metal surface to form a coordinate type of band.[52] The values of ΔG^0_{ads} in our measurements suggest that the adsorption of inhibitors involves both types of interaction chemisorption and physisorption.

Inhibition Efficiency

In general, the inhibition effect of the amides is a result of the adsorption of its molecules on the metal surface. The protection ability of the molecules against corrosion originates from the adsorption of an organic layer.

Amides take protons and have a positive charge in acidic solutions.[46] It is considered that protonizing is effective in amide inhibition. Chloride ions are very active ions and are adsorbed by the IHP (Inner Helmholtz Plane) of the metal, thereby making the metal surface negative. Therefore, the protonated amide molecules may be adsorbed through electrostatic interaction between positively charged amide molecules and the negatively charged metal surface caused by chloride ions from the solution. Neutral amide molecules displace water molecules from the surface and share electrons with the copper surface

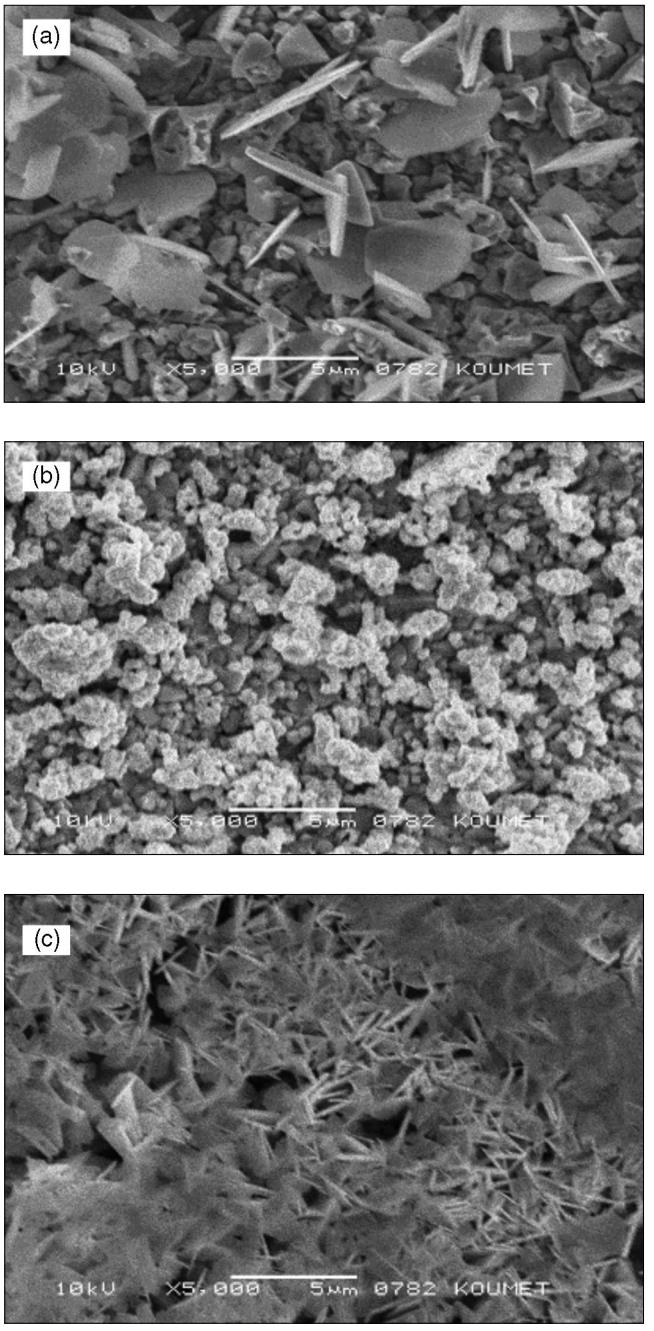


FIGURE 7. *SEM photographs of copper plates kept in 1.0 M HCl solutions, with and without inhibitors, for seven days: (a) 1.0 M HCl, (b) 5 × 10^{-3} M BA, and (c) 5 × 10^{-3} M ABSA.*

$[(Inh)_{sol} + xH_2O_{ads} \leftrightarrow (Inh)_{ads.} + xH_2O_{sol.}]$. In both cases, the adsorbed film protects the surface by blocking mainly the active sites on the copper surface.

Scanning Electron Microscopy Measurements

SEM photographs of copper plates kept in 1.0 M HCl solutions, with and without inhibitors, for 7 days can be seen in Figures 7(a) through (c). Green copper chloride complexes (CuCl, $CuCl_2^-$, $CuCl_3^{2-}$, and $CuCl_4^{3-}$) are covered on the surface of copper, by interacting

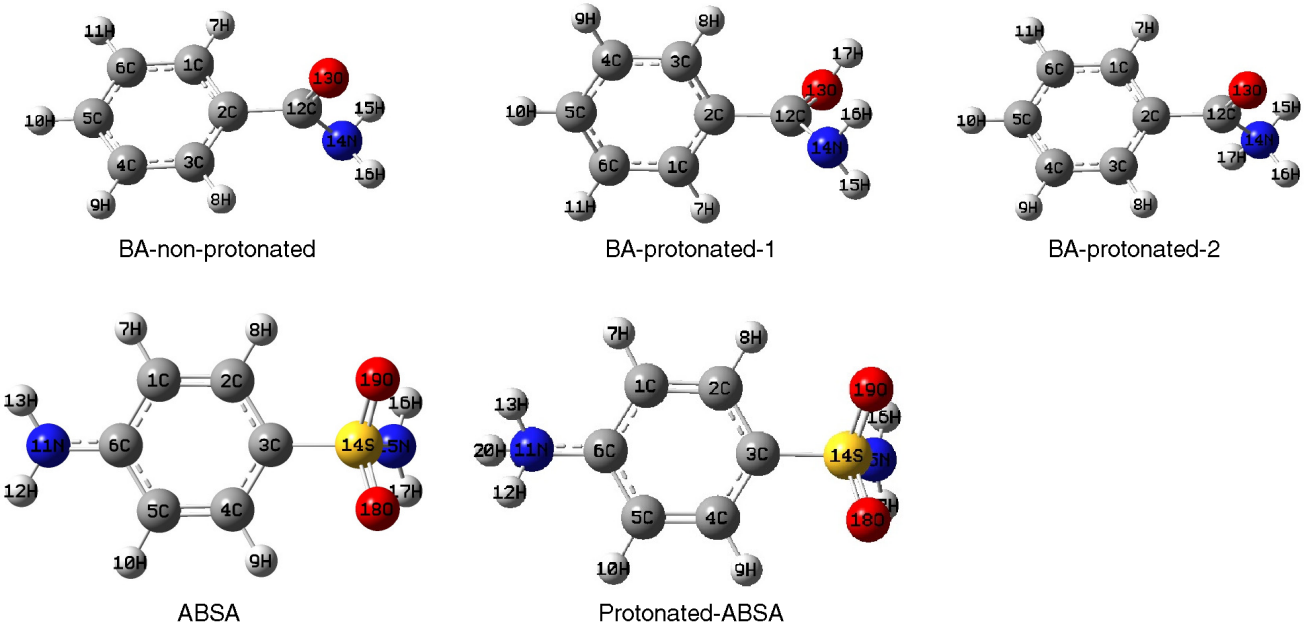


FIGURE 8. *Structure and labeling of a BA, ABSA, both neutral and protonated forms with the labels calculated DFT/B3LYP/6-311++G(2d,2p).*

activated chloride ions with copper ions in 1.0 M HCl solution (Figure 7[a]).[12-13] Inhibitor molecules are covered on the copper surface when inihibitors are added to the chloride solutions and this prevents it from corroding easily. The SEM photographs indicate that the inhibitor molecules are adsorbed on the copper surface (Figures 7[b] and [c]).

Quantum Chemical Calculations

The B3LYP/6-311++G(2d,2p) calculated neutral and protonated forms of BA and ABSA molecules are given in Figure 8.

Figure 9 shows the HOMO population of BA and ABSA and the LUMO population of BA and ABSA.

The HOMO orbitals of the neutral BA and ABSA molecules are concentrated mainly on the aromatic cycle, amide, and sulfonamide groups.

Table 2 represents gas and water phase energy levels (in eV) of the HOMO and LUMO orbitals. The energy gap between E_{HOMO} and E_{LUMO}, dipole moment (μ), molecular volume (MV), sum of the total negative charge (TNC), global hardness (η), softness (σ), chemical potential (π), and electronegativity (χ) values were calculated with B3LYP/6-31G(d,p), B3LYP/6-31++G(2d,2p), MP2/6-31G, and MP2/6-311G levels of theories for the neutral and protonated forms of BA and ABSA molecules. While the LUMO orbital energy indicates the ability of the molecule to accept electrons, HOMO energy is the ability to donate an electron to an appropriate acceptor with empty molecular orbitals. The adsorption and high inhibition efficiency can be related to higher values of E_{HOMO}. The E_{HOMO} value of BA calculated with B3LYP/6-31G(d,p), B3LYP/6-31G++(2d,2p), MP2/6-31G, and MP2/6-311G is –6.72, –7.17, –9.39, and –9.52 eV, respectively, and that of ABSA is –5.98, –6.34, –8.80, and –9.03 eV. As seen from the energies, the E_{HOMO} value of ABSA is higher than BA at all calculated methods, and the ABSA has a higher inhibition efficiency (IE%) value than BA.

Because of being energetically favorable to add electrons to a low-lying LUMO and to receive electrons from a high-lying HOMO, a small HOMO-LUMO energy gap implies low kinetic stability.[45,53] The HOMO-LUMO energy gap of BA calculated at the B3LYP/6-31G(d,p), B3LYP/6-31G ++(2d,2p), MP2/6-31G, and MP2/6-311G levels is 5.73, 5.69, 11.91, and 11.90 eV, respectively. That of ABSA is 5.51, 5.36, 11.48, and 11.43 eV. The HOMO-LUMO energy gap of ABSA is smaller than that of BA, so ABSA has lower kinetic stability than that of BA.

The concepts of absolute electronegativity, absolute hardness, and softness are incorporated into HOMO-LUMO. Hard molecules have a large HOMO-LUMO gap and soft molecules have a small HOMO-LUMO gap.

A small HOMO-LUMO gap means small excitation energies to the manifold of excited states. Therefore, soft molecules, with a small gap, will be more polarizable than hard molecules. High polarizability was the most characteristic property attributed to soft acids and bases.[54] As seen from Table 2, hardness (η) for BA calculated at the B3LYP/6-31G(d,p), B3LYP/6-31G++(2d,2p), MP2/6-31G, and MP2/6-311G levels is 2.865, 2.845, 5.955, and 5.950, respectively, and for ABSA is 2.755, 2.680, 5.740, and 5.715. Softness (σ)

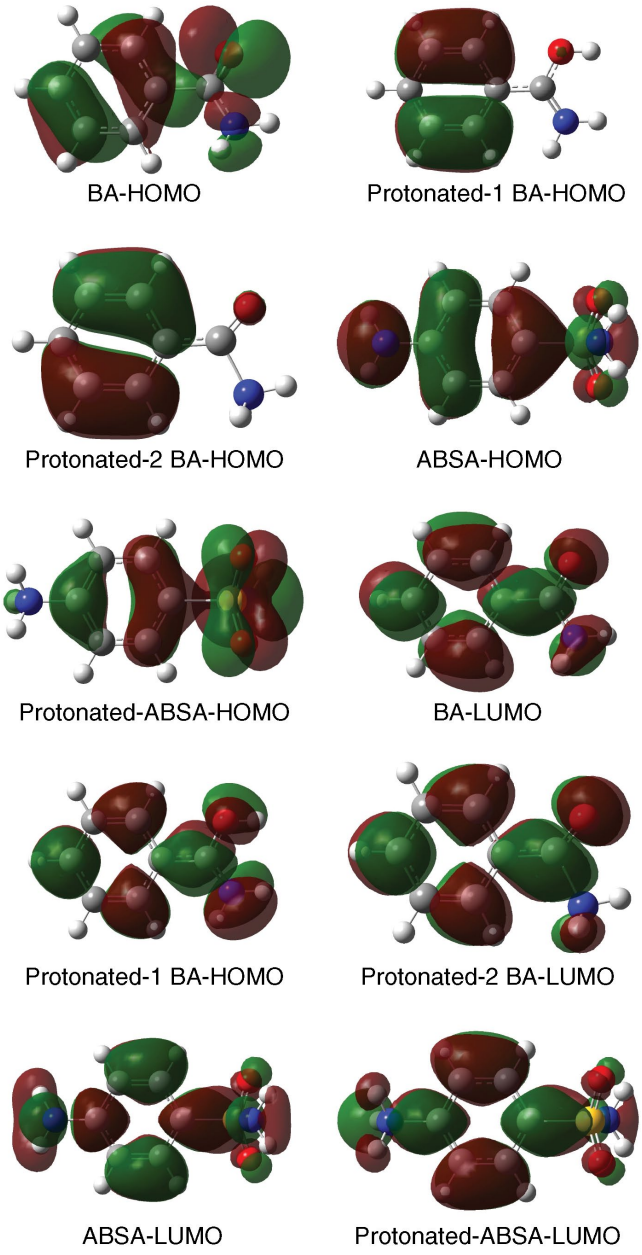


FIGURE 9. *Population of HOMO and LUMO of BA and ABSA with neutral and protonated forms.*

for BA is 0.349, 0.351, 0.168, and 0.168, respectively, and for ABSA is 0.363, 0.373, 0.174, and 0.175 eV.

In addition, cationic species of BA and ABSA were calculated with the same level of theory as neutral molecules. As seen from Table 2, the softness (σ) values of cationic species of BA and ABSA are higher than the neutral counterparts. For example, softness (σ) of BA calculated at the B3LYP/6-31G(d,p) level is 0.349 for neutral BA, whereas 0.430 for protonated BA. Because of the softer molecule being more reactive, the protonated species interact with the metal surface more easily. Similar results have been observed in the literature.[55-59]

Fukui functions allow us to evaluate the nucleophilic and electrophilic behavior of each atom in the molecule.

Fukui functions can be expressed by the following equations:

$$f_k^+ = \rho_k(N+1) - \rho_k(N) \quad \text{(for nucleophilic attack)} \tag{14}$$

$$f_k^- = \rho_k(N) - \rho_k(N-1) \quad \text{(for electrophilic attack)} \tag{15}$$

where k represents the sites (atoms/molecular fragments) for nucleophilic, electrophilic, and radical agents and ρ_k are their gross electron populations. An elevated value of f_k implies a high reactivity of the site k.

The site for nucleophilic attack is controlled by f_k^+ and the site for electrophilic attack is controlled by f_k^-. The values of the Fukui functions for a nucleophilic and electrophilic attack of the BA and ABSA calculated B3LYP/6-31G (d,p) are given for neutral and protonated forms in the gas phase and in the presence of water in Table 3.

For nucleophilic attack, the most reactive site of the BA molecule is on the carbon atoms of the phenyl ring (C1: 12.25%, C2: 18.73%, C3: 8.80%, C4: 5.30%, C5: 22.36%, C6: 2.47%), C12 atom (14.60%), O13 atom (10.52%), and N14 atom (4.27%), As seen from Table 3, these values slightly change in the presence of water. In the protonated form, the reactivity of the phenyl ring decreases (C1: 12.10%, C2: 2.95%, C3: 11.68%, C5: 14.92%), whereas the reactivity of C12 atom increases to 35.93% and N14 to 12.86%. In the ABSA molecule, the most reactive site is mainly on the carbon atom of the phenyl group. In the protonated form, the reactivity slightly changes on the C atom of the phenyl group. In the cationic form, the reactivity of the S atom decreases from 8.05% to 2.62%, and there are changes on the reactivity site of the phenyl ring. As the reactivity of the C1 atom increases from 2.78% to 11.35%, the reactivity of the C2 atom decreases from 12.58% to 6.63% (Table 3).

For electrophilic attack, the most reactive site of the neutral BA molecule is an O atom of the carbonyl group. In the presence of water, the reactivity of the O atom decreases from 60.58% to 34.95% and reactivity on the C atoms of the phenyl ring increases. In the protonated form, the reactivity of the O atom disappears but the reactivity on the C atoms of the phenyl ring appear.

In a neutral ABSA molecule, the most reactive site is mainly collected on the C3 atom of the phenyl ring and N11 atom. The reactive site completely changes at protonated forms. The most reactive site mainly is on the N15 atom (46.20%) and O18 (14.97%), and O19 (14.97%) atoms at protonated ABSA (Table 3).

TABLE 2

Calculated Quantum Chemical Parameters for the BA and ABSA with Neutral and Protonated Forms in the Gas Phase and Water Phase Calculated with Density Functional Theory at the B3LYP/6-31G(d,p) and B3LYP/6-31++G(2d,2p) and MP2/6-31G and MP2/6-311G Basis Set Levels

Molecule	E_{HOMO} (eV)	E_{LUMO} (eV)	ΔE (eV)	μ (D)	MV ($cm^3\ mol^{-1}$)	TNC (e)	η (eV)	σ (eV^{-1})	Pi (eV)	χ (eV)
				B3LYP/6-31G(d,p)						
BA neutral	–6.72	–0.99	5.73	3.497	107.670	–1.523	2.865	0.349	–3.855	3.855
BA neutral[(A)]	–6.82	–0.95	5.87	5.115	101.128	–1.816	2.935	0.341	–3.885	3.885
BA protonated-1	–11.22	–6.57	4.65	5.928	74.042	–1.715	2.325	0.430	–8.895	8.895
BA protonated-1[(A)]	–7.42	–2.24	5.18	8.994	84.545	–1.599	2.590	0.386	–4.830	4.830
BA protonated-2	–11.35	–6.62	4.73	6.374	85.396	–1.361	2.365	0.423	–8.985	8.985
BA protonated-2[(A)]	–7.51	–2.60	4.91	9.214	84.998	–1.558	2.455	0.407	–5.055	5.055
ABSA neutral	–5.98	–0.47	5.51	4.827	131.857	–2.998	2.755	0.363	–3.225	3.225
ABSA neutral[(A)]	–5.75	–0.47	5.28	10.707	105.838	–3.240	2.640	0.379	–3.110	3.110
ABSA protonated	–10.85	–5.31	5.54	16.571	125.397	–2.749	2.770	0.361	–8.080	8.080
ABSA protonated[(A)]	–7.77	–1.58	6.19	24.266	109.692	–2.955	3.095	0.323	–4.675	4.675
				B3LYP/-31G++(2d,2p)						
BA neutral	–7.17	–1.48	5.69	3.663	97.069	–1.905	2.845	0.351	–4.325	4.325
BA neutral[(A)]	–7.20	–1.41	5.79	5.672	89.134	–2.163	2.895	0.345	–4.305	4.305
BA protonated-1	–11.48	–6.87	4.61	5.694	92.008	–1.350	2.305	0.434	–9.175	9.175
BA protonated-1[(A)]	–7.68	–2.55	5.13	8.940	106.697	–1.684	2.565	0.390	–5.115	5.115
BA protonated-2	–11.60	–6.87	4.73	6.268	93.097	–1.531	2.365	0.423	–9.235	9.235
BA protonated-2[(A)]	–7.76	–2.89	4.87	9.245	80.905	–1.744	2.435	0.411	–5.325	5.325
ABSA neutral	–6.34	–0.98	5.36	4.824	112.549	–2.413	2.680	0.373	–3.660	3.660
ABSA neutral[(A)]	–6.08	–0.92	5.16	10.668	112.549	–2.771	2.580	0.388	–3.500	3.500
ABSA protonated	–11.18	–5.60	5.58	16.393	134.145	–1.962	2.790	0.358	–8.390	8.390
ABSA protonated[(A)]	–8.00	–1.88	6.12	24.288	116.388	–2.219	3.060	0.327	–4.940	4.940
				MP2/6-31G						
BA neutral	–9.39	2.52	11.91	4.655	97.139	–2.639	5.955	0.168	–3.435	3.435
BA neutral[(A)]	–9.36	2.59	11.95	4.800	90.528	–2.642	5.975	0.167	–3.385	3.385
BA protonated-1	–13.34	–3.03	10.31	6.765	103.344	–2.541	5.155	0.194	–8.185	8.185
BA protonated-1[(A)]	–13.25	–2.82	10.43	10.004	82.327	–2.531	5.215	0.192	–8.035	8.035
BA protonated-2	–13.51	–3.16	10.35	6.686	105.569	–2.360	5.175	0.193	–8.335	8.335
BA protonated-2[(A)]	–13.37	–3.07	10.30	9.701	87.981	–2.392	5.150	0.194	–8.220	8.220
ABSA neutral	–8.80	2.68	11.48	6.972	131.975	–4.584	5.740	0.174	–3.060	3.060
ABSA neutral[(A)]	–9.00	2.40	11.40	11.501	123.995	–4.574	5.700	0.175	–3.300	3.300
ABSA protonated	–14.17	–2.00	12.17	18.533	113.296	–4.299	6.085	0.164	–8.085	8.085
ABSA protonated[(A)]	–14.23	–2.10	12.13	23.457	137.478	–4.304	6.065	0.165	–8.165	8.165
				MP2/6-311G						
BA neutral	–9.52	2.38	11.90	4.611	121.899	–2.346	5.950	0.168	–3.570	3.570
BA neutral[(A)]	–9.50	2.44	11.94	4.784	97.812	–2.344	5.970	0.168	–3.530	3.530
BA protonated-1	–13.45	–3.07	10.38	6.789	99.296	–2.257	5.190	0.193	–8.260	8.260
BA protonated-1[(A)]	–13.36	–2.84	10.52	10.099	100.074	–2.228	5.260	0.190	–8.100	8.100
BA protonated-2	–13.60	–3.21	10.39	6.841	94.396	–2.096	5.195	0.192	–8.405	8.405
BA protonated-2[(A)]	–13.47	–3.13	10.34	9.856	95.649	–2.142	5.170	0.193	–8.300	8.300
ABSA neutral	–9.03	2.40	11.43	6.722	100.314	–4.043	5.715	0.175	–3.315	3.315
ABSA neutral[(A)]	–9.02	2.38	11.40	7.207	126.393	–4.039	5.700	0.175	–3.320	3.320
ABSA protonated	–14.28	–2.18	12.10	18.511	146.793	–2.824	6.050	0.165	–8.230	8.230
ABSA protonated[(A)]	–14.35	–2.29	12.06	23.723	125.018	–3.815	6.030	0.166	–8.320	8.320

[(A)] In the presence of water.

CONCLUSIONS

❖ Amides (BA and ABSA) are found to be effective inhibitors for copper corrosion in 1.0 M HCl. It was determined that ABSA is more effective than BA.

❖ The corrosion process is inhibited by the adsorption of these molecules on the copper surface. The inhibition efficiency of the BA and ABSA increased with increasing inhibitor concentrations.

❖ Adsorption of the inhibitor fit the Langmuir isotherm model.

❖ The inhibitor behaviors are explained by polarization curves. The inhibitors show mixed-type behavior. However, the decrease in anodic reaction rate is more than the decrease in the cathodic reaction rate.

❖ Current-time measurements at 250 mV indicate that the copper dissolution currents decrease because of the adsorption of inhibitor molecules.

❖ The SEM photograph indicates that the inhibitor molecules are adsorbed on the copper surface.

❖ A quantum chemical study has been performed using the B3LYP functional with the 6-31G(d),

TABLE 3

Fukui Functions and Local Softness Values for a Nucleophilic and Electrophilic for BA and ABSA by B3LYP/6-31G(d,p) Method

	C1	C2	C3	C4	C5	C6	N11	C12	O13	(N/S)14	N15	O18	O19	H20
HOMO														
BA neutral	—	11.07	5.66	—	4.76	5.70	—	3.08	60.58	6.52	—	—	—	—
BA neutral[(A)]	—	16.09	15.34	—	12.59	15.96	—	1.47	34.95	1.60	—	—	—	—
BA protonated-1	26.25	—	27.23	22.36	—	22.91	—	—	—	—	—	—	—	—
BA protonated-1[(A)]	25.27	—	26.23	23.17	—	24.15	—	—	—	—	—	—	—	—
BA protonated-2	22.23	1.91	29.62	17.81	—	26.41	—	—	—	—	—	—	—	—
BA protonated-2[(A)]	20.74	1.58	29.30	18.07	1.30	28.09	—	—	—	—	—	—	—	—
ABSA neutral	13.02	1.54	21.64	1.54	13.02	11.05	30.39	—	—	—	2.98	1.62	1.62	—
ABSA neutral[(A)]	14.05	—	20.60	—	14.09	8.57	34.07	—	—	1.00	3.16	—	—	—
ABSA protonated	—	3.78	6.18	3.78	—	5.50	—	—	—	3.02	46.20	14.97	14.97	3.33
ABSA protonated[(A)]	3.54	8.01	22.79	6.43	4.81	21.61	—	—	—	—	23.08	3.38	3.85	1.57
LUMO														
BA neutral	12.25	18.73	8.80	5.30	22.36	2.47	—	14.60	10.52	4.27	—	—	—	—
BA neutral[(A)]	11.82	17.96	9.69	4.28	22.18	2.76	—	15.68	9.47	5.62	—	—	—	—
BA protonated-1	12.10	2.95	11.68	—	14.92	—	—	35.93	7.65	12.86	—	—	—	—
BA protonated-1[(A)]	11.90	7.00	11.11	1.39	16.40	—	—	30.31	7.23	13.10	—	—	—	—
BA protonated-2	12.43	3.60	12.23	—	15.62	—	—	31.58	21.48	—	—	—	—	—
BA protonated-2[(A)]	11.72	4.89	11.59	—	15.54	—	—	31.54	21.03	—	—	—	—	—
ABSA neutral	2.78	12.58	21.49	12.55	2.79	26.43	6.07	—	—	8.05	1.81	1.55	1.55	—
ABSA neutral[(A)]	1.71	13.90	19.27	13.48	1.85	25.18	7.28	—	—	9.94	3.59	1.53	1.53	—
ABSA protonated	11.35	6.63	25.66	6.63	11.35	25.50	1.34	—	—	2.62	1.19	—	—	—
ABSA protonated[(A)]	7.34	10.55	24.60	10.14	7.73	25.98	—	—	—	5.79	2.52	1.10	1.11	—

[(A)] In the presence of water.

6-311++(2d,2p) basis sets and MP2/6-31G, MP2/6-311G levels. The conclusion obtained by means of the calculation of the HOMO, energy gap ΔE, softness, is the order ABSA > BA, which agrees well with the experiment for all studied levels of theory and basis sets.

ACKNOWLEDGMENTS

The numerical calculations reported in this paper were performed at TUBITAK ULAKBIM, High Performance and Grid Computing Center (TR-Grid e-Infrastructure). The authors would like to thank A. Goksin for grammar and spelling checks.

REFERENCES

1. E.M. Sherif, *Appl. Surf. Sci.* 252 (2006): p. 8615.
2. L. Larabi, O. Benali, S.M. Mekelleche, Y. Harek, *Appl. Surf. Sci.* 253 (2006): p. 1371.
3. M.G. Hosseini, H. Tavakoli, T. Sharabi, *J. Appl. Electrochem.* 38 (2008): p. 1629.
4. K.F. Khaled, *Appl. Surf. Sci.* 255 (2008): p. 1811.
5. E.M. Sherif, S.M. Park, *Electrochim. Acta* 51 (2006): p. 4665.
6. A. Lalitha, S. Ramesh, S. Rajeswari, *Electrochim. Acta* 51 (2005): p. 47.
7. G. Quartarone, M. Battilona, L. Bonaldo, T. Tortato, *Corros. Sci.* 50 (2008): p. 3467.
8. E.M. Sherif, R.M. Erasmus, J.D. Comins, *J. Appl. Electrochem.* 39 (2009): p. 83.
9. K.F. Khaled, N. Hackerman, *Electrochim. Acta* 49 (2004): p. 485.
10. H. Baeza, M. Guzman, P. Ortega, L. Vera, *J. Chil. Chem. Soc.* 48 (2003): p. 23.
11. E.M. Sherif, A.M. El Shamy, M.M. Ramla, A.O.H. El Nazhawy, *Mater. Chem. Phys.* 102 (2007): p. 231.
12. H.P. Lee, K. Nobe, *J. Electrochem. Soc.* 133 (1986): p. 2035.
13. K.F. Khaled, *Mater. Chem. Phys.* 112 (2008): p. 104.
14. D.Q. Zhang, L. Gao, G. Zhou, *Appl. Surf. Sci.* 252 (2006): p. 4975.
15. D.Q. Zhang, L. Gao, G. Zhou, *Appl. Surf. Sci.* 225 (2004): p. 287.
16. D.Q. Zhang, L. Gao, G. Zhou, K.Y. Lee, *J. Appl. Electrochem.* 38 (2008): p. 71.
17. D.Q. Zhang, C. Qi-Rui, H. Xian-Ming, G. Li-Xin, K.G. Soon, *Corros. Sci.* 51 (2009): p. 2349.
18. M.M. Antonijevic, M.B. Petrovic, *Int. J. Electrochem.* 3 (2008): p. 1.
19. L. Tommesani, G. Brunoro, A. Frignani, C. Monticelli, M. Dalcolle, *Corros. Sci.* 39 (1997): p. 1221.
20. D. Jope, J. Sell, H.W. Pickering, K.G. Weil, *J. Electrochem. Soc.* 142 (1995): p. 2170.
21. R. Youda, H. Nishihara, K. Aramaki, *Corros. Sci.* 28 (1988): p. 87.
22. A.M. Fenelon, C.B. Breslin, *J. Appl. Electrochem.* 31 (2001): p. 509.
23. T. Notoya, G.W. Poling, *Corrosion* 32 (1976): p. 216.
24. D.Q. Zhang, L. Gao, G. Zhou, *J. Appl. Electrochem.* 35 (2005): p. 1081.
25. D.Q. Zhang, Q. Cai, X.M. He, L.X. Gao, G.S. Kim, *Mater. Chem. Phys.* 114 (2009): p. 612.
26. O.L. Riggs, C.C. Nathan, *Corrosion Inhibitors*, 2nd ed. (Houston, TX: NACE International, 1973), p. 7-28.
27. K.M. Ismail, *Electrochim. Acta* 52 (2007): p. 7811.
28. A.C. Makrides, N. Hackermann, *J. Phys. Chem.* 59 (1955): p. 707.
29. M. Ozcan, F. Karadag, I. Dehri, *Colloids Surf. A: Physicochem. Eng. Aspects* 316 (2008): p. 55.
30. F. Kandemirli, S. Sagdinc, *Corros. Sci.* 49 (2007): p. 2118.
31. S. Zor, F. Kandemirli, M. Bingul, *Prot. Met. Phys. Chem. Surf.* 45 (2009): p. 46.
32. E.E. Ebenso, T. Arslan, F. Kandemirli, N. Caner, I. Love, *Int. J. Quantum Chem.* 110 (2010): p. 1003.
33. S. Zor, F. Kandemirli, E. Yakar, T. Arslan, *Prot. Met. Phys. Chem. Surf.* 46 (2010): p. 110.
34. S. Zor, H. Ozkazanc, T. Arslan, F. Kandemirli, *Corrosion* 66 (2010): p. 045006-1, doi:10.5006/1.3381571.
35. M.J. Frisch, G.W. Trucks, H.B. Schlegel, G.E. Scuseria, M.A. Robb, J.R. Cheeseman, G. Scalmani, V. Barone, B. Mennucci, G.A. Petersson, H. Nakatsuji, M. Caricato, X. Li, H.P. Hratchian, A.F. Izmaylov, J. Bloino, G. Zheng, J.L. Sonnenberg, M. Hada, M. Ehara, K. Toyota, R. Fukuda, J. Hasegawa, M. Ishida, T. Nakajima, Y. Honda, O. Kitao, H. Nakai, T. Vreven, J.A. Montgomery, Jr., J.E. Peralta, F. Ogliaro, M. Bearpark, J.J. Heyd, E. Brothers, K.N. Kudin, V.N. Staroverov, R. Kobayashi, J. Normand, K. Raghavachari, A. Rendell, J.C. Burant, S.S. Iyengar, J. Tomasi, M. Cossi, N. Rega, J.M. Millam, M. Klene, J.E. Knox, J.B. Cross, V. Bakken, C. Adamo, J. Jaramillo, R. Gomperts, R.E. Stratmann, O. Yazyev, A.J. Austin, R. Cammi, C. Pomelli, J.W. Ochterski, R.L. Martin, K. Morokuma, V.G. Zakrzewski, G.A. Voth, P. Salvador, J.J. Dannenberg, S. Dapprich, A.D. Daniels, Ö. Farkas, J.B. Foresman, J.V. Ortiz, J. Cioslowski, D.J. Fox, Gaussian 09, Revision A.1, Gaussian, Inc., Wallingford, CT, 2009.
36. G.A. Petersson, A. Bennett, T.G. Tensfeldt, M.A. Al-Laham, W.A. Shirley, J. Mantzaris, *J. Chem. Phys.* 89 (1988): p. 2193.

37. A.D. Becke, *J. Chem. Phys.* 98 (1993): p. 5648.
38. J.M. Costa, J.M. Llush, *Corros. Sci.* 24 (1984): p. 929.
39. C. Lee, W. Yang, R.G. Parr, *Phys. Rev. B* 41 (1988): p. 785.
40. S.I. Gorelsky, AOMix: Program for Molecular Orbital Analysis, University of Ottawa, Ottawa, Canada, 2009, http://www.sg-chem.net.
41. S.I. Gorelsky, A.B.P. Lever, *J. Organomet. Chem.* 635 (2001): p. 187.
42. F.K. Crundwell, *Electrochim. Acta* 37 (1992): p. 2707.
43. V. Brusic, M.A. Frisch, B.N. Eldridge, F.P. Novak, F.B. Kaufman, B.M. Rush, G.S. Frankel, *J. Electrochem. Soc.* 138 (1991): p. 2253.
44. A.L. Bacarella, J.C. Griess, *J. Electrochem. Soc.* 120 (1973): p. 459.
45. G.W. Poling, *Corros. Sci.* 10 (1970): p. 359.
46. E.E. Ebenso, U.J. Ekpe, B.I. Ita, O.E. Offiong, U.J. Ibok, *Mater. Chem. Phys.* 60 (1999): p. 79.
47. A. Yurt, S. Ulutas, H. Dal, *Appl. Surf. Sci.* 253 (2006): p. 919.
48. A.R. Yazdzad, T. Shahrabi, M.G. Hosseini, *Mater. Chem. Phys.* 109 (2008): p. 199.
49. K.F. Khaled, M.M. Al-Qahtani, *Mater. Chem. Phys.* 113 (2009): p. 150.
50. M. Hosseini, S.F.L. Mertens, M.R. Arshadi, *Corros. Sci.* 45 (2003): p. 1473.
51. A. Popova, E. Sokolova, S. Raicheva, M. Christov, *Corros. Sci.* 45 (2003): p. 33.
52. C. Küstü, K.C. Emregül, O. Atakol, *Corros. Sci.* 49 (2007): p. 2800.
53. G. Moretti, F. Guidi, *Corros. Sci.* 44 (2002): p. 1995.
54. R.G. Pearson, *Proc. Nati. Acad. Sci.* 83 (1986): p. 8440.
55. B. Gomez, N.V. Likhanova, M.A. Dominguez-Aguilar, R. Martinez-Palou, A. Vela, J.L. Gasquez, *J. Phys. Chem. B* 110 (2006): p. 8928.
56. E.E. Ebenso, T. Arslan, F. Kandemirli, N. Caner, I. Love, C. Ogretir, M. Saracoglu, *Int. J. Quantum Chem.* 110 (2010): p. 2614.
57. T. Arslan, F. Kandemirli, E.E. Ebenso, I. Love, H. Alemu, *Corros. Sci.* 51 (2009): p. 35.
58. M.A. Amin, M.A. Ahmed, H.A. Arida, T. Arslan, M. Saracoglu, F. Kandemirli, *Corros. Sci.* 53 (2011): p. 540.
59. M.A. Amin, M.A. Ahmed, H.A. Arida, F. Kandemirli, M. Saracoglu, T. Arslan, M.A. Basaran, *Corros. Sci.* 53 (2011): p. 1895.